



Research Article

ISSN : 0975-7384
CODEN(USA) : JCPRC5

Synthesis, structural characterization, electrochemical, biological, antioxidant and nuclease activities of 3-morpholinopropyl amine mixed ligand complexes

Jeyaraj Dhaveethu Raja^a, Gurusamy Sankararaj Senthilkumar^{b,d}, Chinnapiyan Vedhi^c and Manokaran Vadivel^a

^aChemistry Research Centre, Mohamed Sathak Engineering College, Kilakarai, Ramanathapuram (Dist), Tamilnadu, India

^bDepartment of Chemistry, Sri Vidya College of Engineering & Technology, Virudhunagar, Tamilnadu, India

^cPG & Research Department of Chemistry, V. O. Chidambaram College, Thoothukudi, Tamilnadu, India

^dManonmaniam Sundaranar University, Tirunelveli, Tamilnadu, India

ABSTRACT

A new series of water-soluble transition mixed ligand complexes of Co (II) and Ni (II) have been synthesized from the Schiff base ligand (HL) derived from morpholine derivatives as a primary ligand with 1,10-phenanthroline (X) and 2,2'-bipyridine (Y) as co-ligands. Structural features were obtained from their elemental analyses, magnetic susceptibility, molar conductance, mass, FT-IR, UV-Vis., spectral studies. The data show that all the mixed ligand complexes have composition of [MLX]4H₂O and [MLY]4H₂O. The spectral data showed octahedral geometry around the central metal ion. The redox behavior of metal complexes was studied by cyclic voltammetry. The binding strength and binding mode of complexes with HS DNA (Herring Sperm) have been investigated by absorption titration and viscosity measurement studies. The results show a considerable interaction between complexes and HS-DNA. The nuclease activities of the complexes have shown that they cleave calf thymus DNA under aerobic condition and in the presence of H₂O₂ through redox chemistry. The in vitro biological and antioxidant activities have shown that the mixed ligand complexes have higher potent activities than the free ligand.

Keywords: Morpholine, Schiff base, Antioxidant, DNA binding, DNA cleavage.

INTRODUCTION

Schiff base complexes are used as ligand because of the combination of molecular nitrogen with central metal ions and also it has been reported to possess antimicrobial properties [1-4]. Morpholine derivatives were reported to possess antimicrobial [5-6] anti-inflammatory [7-9] and central nervous system activities [10-11]. The heterocyclic compounds exhibit biological activities due to the presence of multifunctional groups. Most of them have N, O and S containing groups which form strain-free five or six-membered ring and give 1:1 (M-L) chelate with metal ions such as Ni (II) and Co (II). Metal complexes exhibit interactions with DNA have been studied with the aims of developing both probes for nucleic acid structures and chemotherapy agents [12]. Bidentate ligand, such as 2,2'-bipyridine, 1,10-phenanthroline readily form complexes with most of the transition metal ions. These have been extensively used in both biological and preparative coordination chemistry [13-15]. Transition metal complexes have been adopted for their spectral, electrochemical properties and ability to change the ligand environment while binding and cleaving with DNA. These studies are also important in determining the pathway of metal ion toxicity [16-17]. The aromatic rings of the ligands were used to stack the bases of DNA. The existence of oxygen and nitrogen atoms that can create hydrogen bonds with the DNA, and the metal complexes show a positive charge so as to interact electrostatically with phosphate groups of DNA. Generally, metal complexes capable of abstracting ribosyl hydrogen are expected to oxidize guanine or other nucleobases. Current efforts are carried out to design mixed ligand complexes as chemical nucleases suitable for direct strand scission. The interaction studies between

complexes and DNA is one of the most important aspects in biological research aimed at discovering and developing new type of anti- proliferative agents [18] because DNA is one of the main molecular targets in the design of anticancer compounds [19]. The practical use of transition metal complexes as chemical nuclease is also documented [20-21]. Hence, we have explored the synthesis, characterization, biological, electrochemical, radical scavenging, DNA binding and cleavage studies of mixed ligand complexes containing tridentate schiff base.

EXPERIMENTAL SECTION

All reagents 3-morpholinopropylamine, salicylaldehyde, metal(II) salts and DPPH used were extra pure AR grade (Sigma/Aldrich) and used without further purification. Solvents were used for physical measurements are of AR grade and purified by standard methods [22]. Triply distilled water (specific conductance = $1.81 \pm 0.1 \text{ } \Lambda^{-1} \text{ cm}^{-1}$) was stored in a CO₂ free atmosphere and was used for solution preparations. Melting points of all the mixed ligand complexes were determined on Gallen kamp apparatus in open glass capillaries and were uncorrected. The elemental analysis of carbon, hydrogen and nitrogen were recorded in an Elementar Vario EL III, CHNS analyser at STIC, CUSAT, India. Molar conductance of the complexes was measured in EtOH solvent using 305 systronic conductivity bridge by using 0.01 M KCl solutions as calibrant. The mass spectra were analyzed by FAB & ESI-MS spectrum in a 3-nitro-benzylalcohol matrix. Magnetic susceptibility measurement on power samples was carried out by the Gouy method using Hg[Co(SCN)₄] as calibrant and the diamagnetic corrections were applied in compliance with Pascal's constant. Electronic absorption spectra of the complexes in ethanol medium were recorded on a Shimadzu UV1800 spectrometer (path length, 1 cm) 100-1000nm range. IR spectra were recorded using KBr pellet on a Shimadzu FT-IR affinity spectrometer in 4000 – 400 cm⁻¹ range and Electrochemical studies were carried out using electrochemical analyser model CHI620C. Cyclic voltammetric measurements were performed using a glassy carbon working electrode (3 mm dia), Pt wire auxiliary electrode and an Ag/AgCl reference electrode. All solutions were purged with N₂ for 30 min prior to each set of experiments. Tetrabutylammonium perchlorate TBAP was used as the supporting electrolyte. The magnetic susceptibility data of the complexes were obtained with a Gouy balance at room temperature using copper sulphate as a calibrant. Calf thymus DNA was purchased from Gene (India). Viscosity experiments were carried on an Ubbelodhe viscometer, immersed in a thermostated water-bath maintained at $30 \pm 0.1^\circ\text{C}$. The CT-DNA Cleavage, HS-DNA binding and antioxidant studies were recorded in EtOH solution using UV-Transilluminator, and 1800 UV-Visible spectrophotometer in DST-SERB sponsored Research lab, Chemistry Research Centre, MSEC, Kilakarai, Ramanathapuram, Tamilnadu, India.

2.2 Synthesis of Schiff base [HL]

An ethanolic solution (20 ml) of 3-morpholinopropylamine (1.44 g, 10 mmol) and salicylaldehyde (1.22 g, 10 mmol) were reflux for 3h. The resulting solution was evaporated slowly to separate solvent completely from reaction mixture. On cooling, the yellow orange liquid of 2-(3-morpholinopropylimino) methyl phenol (Figure 1) was formed then purified by column chromatography with petroleum ether and methanol solvent mixture.

[HL]: [Yield: 2.1 g, 79 %] Analysis: calculated for C₁₄H₂₀N₂O₂: C, 67.7; H, 8.1; N, 11.3 %. Found: C, 67.1; H, 8.9; N, 11.7 %; FAB-MS (relative abundance, %): m/z 248; IR (KBr, cm⁻¹): 3210 v(O-H phenolic), 1630 v(-CH=N), 1200 v(C-O Phenolic), 1143 v(C-O aliphatic), 1338 v(C-N aliphatic), 3056 v(C-H aromatic), 2949 v(C-H aliphatic), 2852 v(C-H iminic); UV-Vis in EtOH (λ_{max} /nm): 399, 315, 254.

2.3 Synthesis of metal complexes with 1,10-phenanthroline [MLX]4H₂O

A solution of the LH (0.124 g, 0.5 mmol) in ethanol (20 ml) was added to a solution of metal salts like [Co(Ac)₂].4H₂O and [Ni(Ac)₂].4H₂O (0.5 mmol) in 20 ml ethanol and the mixture was refluxed for ca. 4 h. An ethanolic solution of 1,10-phenanthroline (X) (0.090 g, 0.5 mmol) was mixed and refluxed for 2 h. The resulting solution then concentrated to one third and kept at room temperature for 48 h. The solid complexes were formed washed thoroughly with ethanol and dried in vacuum desiccator. All the complexes were recrystallized from ethanol.

[CoLX]4H₂O: [Yield: 0.20 g, 60 %] Analysis: calculated for CoC₂₈H₃₈N₄O₈: C, 54.5; H, 6.2; N, 9.1 %. Found: C, 54.4; H, 6.1; N, 9.1 %; FAB-MS (relative abundance, %): m/z 617; IR (KBr, cm⁻¹): 1620 v(-CH=N); 1401 v(acetate), 1223 v(C-O Phenolic), 1143 v(C-O aliphatic), 1338 v(C-N aliphatic), 3067 v(C-H aromatic), 2955 v(C-H aliphatic), 2850 v(C-H iminic), 1570 v(C-N phenanthroline), 860 v(H₂O), 653 v(M-O), 492 v(M-N); UV-Vis in EtOH (λ_{max} /nm): 980, 612, 399; Conductance in EtOH (Λ_{M}): 21.2 ohm⁻¹cm mol⁻¹; Magnetic moment, μ_{eff} (BM): 4.8.

[NiLX]4H₂O: [Yield: 0.13 g, 59 %] Analysis: calculated for NiC₂₈H₃₈N₄O₈: C, 54.5; H, 6.2; N, 9.1 %. Found: C, 54.2; H, 6.2; N, 9.0 %; FAB-MS (relative abundance, %): m/z 617; IR (KBr, cm⁻¹): 1622 v(-CH=N); 1404 v(acetate), 1229 v(C-O Phenolic), 1139 v(C-O aliphatic), 1349 v(C-N aliphatic), 3050 v(C-H aromatic), 2956 v(C-H

aliphatic), 2856 $\nu(\text{C-H iminic})$, 1558 $\nu(\text{C-N phenanthroline})$, 845 $\nu(\text{H}_2\text{O})$, 659 $\nu(\text{M-O})$, 483 $\nu(\text{M-N})$; UV-Vis in EtOH ($\lambda_{\text{max}}/\text{nm}$): 942, 548, 418; Conductance in EtOH (Λ_{M}): $19.6 \text{ ohm}^{-1} \text{ cm}^2 \text{ mol}^{-1}$; Magnetic moment, μ_{eff} (BM): 3.1.

2.4 Synthesis of metal complexes with 2,2'-bipyridine [MLY]4H₂O

A solution of the LH (0.124 g, 0.5 mmol) in ethanol (20 ml) was added to a solution of metal salts like [Co(Ac)₂]₄H₂O and [Ni(Ac)₂]₄H₂O (0.5mmol) in 20 ml ethanol and the mixture was refluxed for ca. 4 h. An ethanolic solution of 2,2'-bipyridine (Y) (0.0781 g, 0.5 mmol) was mixed and refluxed for 2 h. The resulting solution then concentrated to one third and kept at room temperature for 48 h. The solid complexes were formed washed thoroughly with ethanol and dried in vacuum desiccators. All the complexes were recrystallized from ethanol.

[CoLY]4H₂O: [Yield: 0.18 g, 59 %] Analysis: calculated for CoC₂₆H₃₈N₄O₈: C, 52.6; H, 6.4; N, 9.4 %. Found: C, 52.5; H, 6.6; N, 9.5 %; FAB-MS (relative abundance, %): m/z 593; IR (KBr, cm^{-1}): 1598 $\nu(\text{-CH=N})$; 1399 $\nu(\text{acetate})$, 1232 $\nu(\text{C-O Phenolic})$, 1140 $\nu(\text{C-O aliphatic})$, 1340 $\nu(\text{C-N aliphatic})$, 3065 $\nu(\text{C-H aromatic})$, 2943 $\nu(\text{C-H aliphatic})$, 2848 $\nu(\text{C-H iminic})$, 1569 $\nu(\text{C-N bipyridine})$, 855 $\nu(\text{H}_2\text{O})$, 617 $\nu(\text{M-O})$, 497 $\nu(\text{M-N})$; UV-Vis in EtOH ($\lambda_{\text{max}}/\text{nm}$): 987, 617, 410; Conductance in EtOH (Λ_{M}): $19.4 \text{ ohm}^{-1} \text{ cm}^2 \text{ mol}^{-1}$; Magnetic moment, μ_{eff} (BM): 4.7.

[NiLY]4H₂O: [Yield: 0.17 g, 57 %] Analysis: calculated for NiC₂₆H₃₈N₄O₈: C, 52.6; H, 6.4; N, 9.4 %. Found: C, 52.7; H, 6.3; N, 9.7 %; FAB-MS (relative abundance, %): m/z 593; IR (KBr, cm^{-1}): 1616 $\nu(\text{-CH=N})$; 1400 $\nu(\text{acetate})$, 1229 $\nu(\text{C-O Phenolic})$, 1139 $\nu(\text{C-O aliphatic})$, 1344 $\nu(\text{C-N aliphatic})$, 3069 $\nu(\text{C-H aromatic})$, 2941 $\nu(\text{C-H aliphatic})$, 2849 $\nu(\text{C-H iminic})$, 1565 $\nu(\text{C-N bipyridine})$, 840 $\nu(\text{H}_2\text{O})$, 657 $\nu(\text{M-O})$, 487 $\nu(\text{M-N})$; UV-Vis in EtOH ($\lambda_{\text{max}}/\text{nm}$): 975, 607, 380; Conductance in EtOH (Λ_{M}): $21.2 \text{ ohm}^{-1} \text{ cm}^2 \text{ mol}^{-1}$; Magnetic moment, μ_{eff} (BM): 3.3.

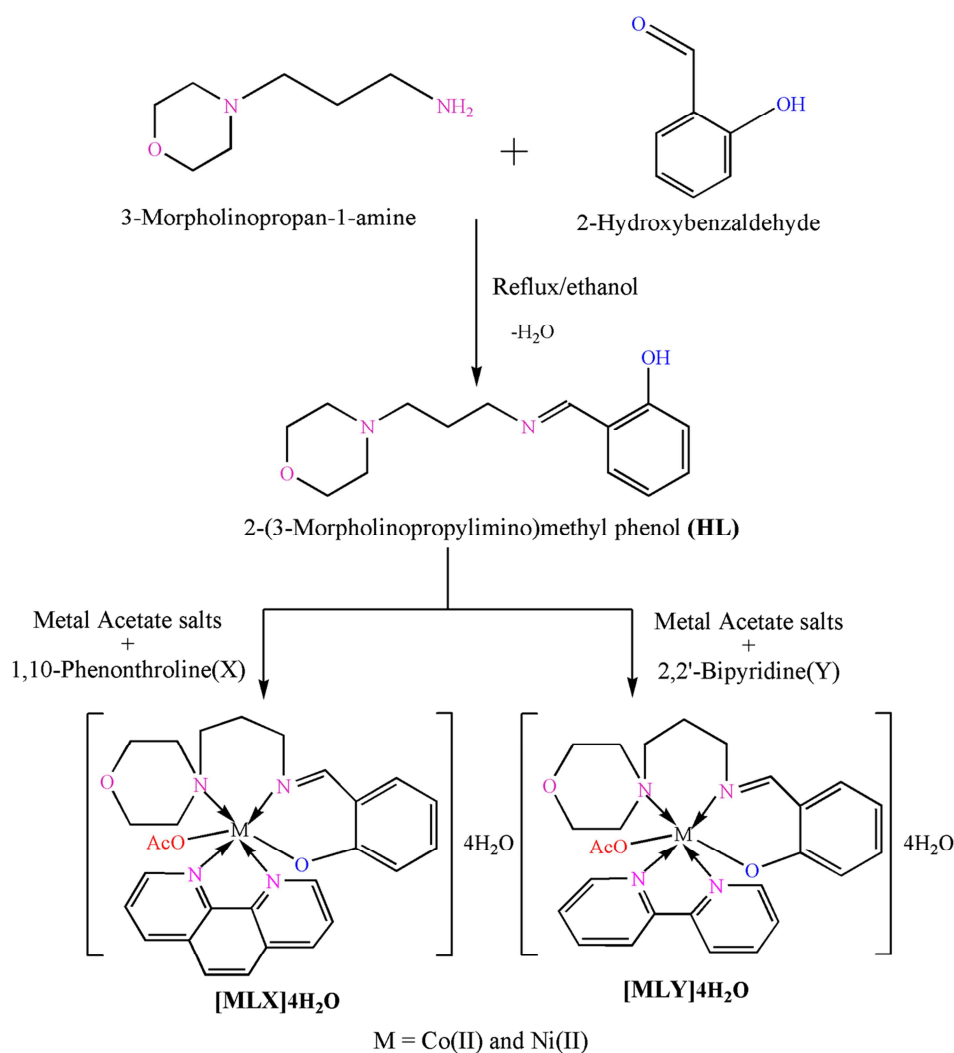


Figure 1 Synthesis of schiff base ligand and its mixed ligand complexes

2.5 DNA binding Studies

2.5.1 Absorption method

All the experiments involving the interaction of the complexes with herring sperm (HS) DNA were carried out in Tris-HCl buffer (50 mM NaCl/5 mM Tris-HCl, pH 7.1) at room temperature. A solution of HS DNA in the buffer gave a ratio of UV absorbance at 260 and 280 nm of about 1.8-1.9, indicating that DNA was sufficiently free from protein [23]. The HS-DNA concentration per nucleotide was determined by absorption spectroscopy using the molar absorption coefficient of $6600 \text{ M}^{-1} \text{ cm}^{-1}$ at 260 nm [24]. The compounds were dissolved in a mixed solvent of 5% methanol and 95% Tris-HCl buffer for all the experiments. Stock solutions were stored at 4°C and used within 4 days. Absorption titration experiments were performed with fixed concentration of the compounds ($30 \mu\text{M}$) with varying concentration of DNA ($0\text{--}60 \mu\text{M}$). The absorption spectra have measured by an equal amount of DNA was added to all the test solutions and the reference solution to eliminate the absorbance of DNA itself [25].

2.5.2 Viscosity measurements

Cannon-Ubbelodhe viscometer maintained at a constant temperature of $27.0 \pm 0.1^\circ \text{C}$ in a thermostatic jacket was used to measure the relative viscosity of DNA solutions. A 3.0 mM stock solution of each ethidium bromide was prepared. A 0.4 mM solution of HS DNA was used. The $[\text{Complex}]/[\text{DNA}]$ ratio was maintained in the range $0\text{--}0.2$. Flow time was measured with a digital stopwatch with an accuracy of 0.01 s . The flow time of each sample was measured three times and an average flow time was calculated. Data were represented graphically as $(\eta/\eta_0)^{1/3}$ versus concentration ratio ($[\text{Complex}]/[\text{DNA}]$), where η is viscosity of DNA in the presence of complex and η_0 is viscosity of DNA alone [26]. Viscosity values were calculated from the observed flow time of DNA-containing solutions ($t > 100 \text{ s}$) corrected for the flow time of buffer alone (t_0) i.e. $\eta \propto t - t_0$.

2.6 DNA cleavage Studies

The DNA cleavage experiment was conducted using CT-DNA by gel electrophoresis with the corresponding metal complex in the presence of H_2O_2 as an oxidant. The reaction mixture was incubated before electrophoresis experiment at 35°C for 2 h as follows: CT DNA $30 \mu\text{M}$, $50 \mu\text{M}$ each complex, $50 \mu\text{M}$ H_2O_2 in 50 mM Tris-HCl buffer (pH = 7.2). The samples were electrophoresed for 2 h at 50 V on 1% agarose gel using Tris-acetic acid-EDTA buffer (pH = 7.2). After electrophoresis, the gel was stained using $1 \mu\text{g}/\text{cm}^3$ ethidium bromide and photographed under UV light.

2.7 In vitro Antioxidant activity

All the mixed ligand complexes were tested for *in vitro* antioxidant activities at 37°C by DPPH free radical scavenging assay method as prepared by Blois [27]. Solutions of mixed ligand complexes at different concentrations ($10, 20, 30, 40$ and $50 \mu\text{M}$) were prepared in EtOH solvent. 1 mL of each sample solution having different concentrations and 4 mL of 0.1 mM DPPH solution were taken in different test tubes and the mixture was shook vigorously for about 2-3 min. Then test tubes were incubated in dark room for 20-30 min at 37°C . A blank DPPH solution without the sample was used for the baseline correction and it gives a strong absorption maximum at 517 nm (purple color with $\epsilon = 8.32 \times 10^3 \text{ M}^{-1} \text{ cm}^{-1}$). After incubation, the absorbance value for each sample $510\text{--}520 \text{ nm}$ was measured using a UV-visible spectrometer. The observed decrease in the absorbance values indicate that the mixed ligand complexes show scavenging activity. Free radical scavenging effects in percentage was calculated using the formula:

$$\text{Scavenging effects (\%)} = \left[\frac{(A_{\text{control}} - A_{\text{sample}})}{A_{\text{control}}} \right] \times 100$$

Where A_{control} is the absorbance of the control (blank) and A_{sample} is the absorbance of the complex. All the analyses were made in three replicate for each and this results were compared with each other.

2.8 In vitro biological study

2.8.1 Antibacterial activity

NCCLS approved standard nutrient agar was used as medium for testing the activity of microorganisms as antibacterial agents. For preparing the agar media, 3 g of beef extract, 5 g of peptone, 5 g of yeast extract and 5 g of sodium chloride were dissolved in 1000 mL of distilled water in a clean conical flask. The pH of the solution was maintained at 7.0 . The solution was boiled to dissolve the medium completely and sterilized by autoclaving at 15 lbs pressure (120°C) for 30 min . After sterilization, 20 mL of media was poured into the sterilized petri plates. These petri plates were kept at room temperature for some time. After few minutes the medium got solidified in the plates. Then, it was inoculated with microorganisms using sterile swabs. The stock solutions were prepared by dissolving the compounds in ethanol at $1 \times 10^{-2} \text{ M}$ to find the inhibition zone values. In a typical procedure, a well was made on the agar medium inoculated with microorganisms [28]. The well was filled with the test solutions using a

micropipette and the plates were incubated at 37 °C for 24 h. During this period, the test solution diffused and affected the growth of the inoculated bacteria. The inhibition zone was developed and it was noted in mm.

2.8.2 Antifungal activity

NCCLS approved standard potato dextrose agar was used as medium for antifungal activity by well diffusion method. For preparing the agar media, 200 g of potato extract, 20 g of agar and 20 g of dextrose were dissolved in 1000 ml of distilled water in a clean conical flask. The solution was boiled to dissolve the medium completely and sterilized by autoclaving at 15 lbs. pressure (120 °C) for 30 min. After sterilization, 20 ml of media was poured into the sterilized Petri plates. These Petri plates were kept at room temperature for some time. After few minutes the medium got solidified in the plates. Then, it was inoculated with microorganisms using sterile swabs. The stock solutions were prepared by dissolving the compounds in ethanol at 10^{-2} M to find the inhibition zone values. In a characteristic procedure, a well was made on the agar medium inoculated with microorganisms [29]. The well was filled with the test solutions using a micropipette and the plates were incubated at 37°C for 72 h. During this period, the test solution diffused and affected the growth of the inoculated fungi. The inhibition zone was developed and it was noted in mm.

RESULTS AND DISCUSSION

All the mixed ligand complexes are hygroscopic in nature. They are soluble in water, ethanol, methanol, chloroform and insoluble in petroleum ether and hexane. The micro-analytical data for the synthesized complexes show that the metal to primary ligand and co-ligand ratio is 1:1:1. The observed molar conductance of the complexes in EtOH (10^{-3} M) at room temperature is constituent with the non-electrolytic nature of the complexes and in the absence of counter ions in the proposed structure of the metal complexes [30]. Figure 1 shows the structure of ligand and synthesized mixed ligand complexes. The physical properties of the complexes are summarized in Table 1. The analytical data correspond well with the general formula of complexes like $[MLX]4H_2O$ and $[MLY]4H_2O$.

3.1 Mass spectroscopy

The observed molecular ion peak confirms the proposed formulae and is in good agreement with their theoretical molecular weight as calculated from micro-analytical data. The Schiff base ligand [HL] showed a molecular ion peak at m/z 248 which was also supported by the 'nitrogen rule', since the compound possesses two nitrogen atoms. The molecular ion peaks for the $[CoLX]4H_2O$ and $[CoLY]4H_2O$ complexes have observed at m/z 617 and 593 confirms the stoichiometry of metal chelates as $[MLX]4H_2O$ type.

Table 1 Physical characterization, analytical, molar conductance and magnetic susceptibility data of the ligand and the complexes

Compound	Molecular formula	Colour	Yield (%)	Found (Calcd.) (%)				Molar Conductance \wedge^m (ohm ⁻¹ cm mol ⁻¹)	μ_{eff} (BM)
				M	C	H	N		
[HL]	C ₁₄ H ₂₀ N ₂ O ₂	Orange	79	----	67.1 (67.7)	8.9 (8.1)	11.7 (11.3)	----	----
[CoLX]4H ₂ O	CoC ₂₈ H ₃₈ N ₄ O ₈	Dark Pink	60	9.8 (9.6)	54.4 (54.5)	6.1 (6.2)	9.1 (9.1)	21.2	4.8
[NiLX]4H ₂ O	NiC ₂₈ H ₃₈ N ₄ O ₈	Pale Green	59	9.4 (9.6)	54.2 (54.2)	6.2 (6.2)	9.0 (9.1)	19.6	3.1
[CoLY]4H ₂ O	CoC ₂₆ H ₃₈ N ₄ O ₈	Dark Pink	59	9.9 (10.0)	52.5 (52.6)	6.6 (6.4)	9.5 (9.4)	19.4	4.7
[NiLY]4H ₂ O	NiC ₂₆ H ₃₈ N ₄ O ₈	Pale Green	57	10.2 (10.0)	52.7 (52.6)	6.3 (6.4)	9.7 (9.4)	21.2	3.3

3.2 Electronic absorption spectroscopy

The electronic absorption spectra of the ligand, and its mixed ligand complexes were recorded in ethanol at 300 K. Ligand is showed two intra ligand charge transfer (INCT) transition bands for phenyl ring and the azomethine chromophore (-CH=N). In the metal complexes this bands are shifted to a longer wavelength which is attributed to the donation of lone pair electron of nitrogen atom of the ligand to the metal (N→M). The electronic spectrum (Figure 2) of $[CoLX]4H_2O$ complex is showed three d-d bands which are assigned as $^4T_{1g}(F) \rightarrow ^4T_{2g}(F)$ ν_1 (10204 cm⁻¹), $^4T_{1g}(F) \rightarrow ^4A_{2g}(F)$ ν_2 (16340 cm⁻¹) and $^4T_{1g}(F) \rightarrow ^4T_{1g}(P)$ ν_3 (25062 cm⁻¹) d-d transitions respectively, which are strongly favoured for the octahedral geometry [31-37] and also the observed magnetic moment value of Co (II) complex is 4.7-5.2 BM (paramagnetic), which is confirmed the octahedral geometry. Similarly, the spectrum of $[NiLX]4H_2O$ complex is showed three d-d bands which are assigned as $^3A_{2g}(F) \rightarrow ^3T_{2g}(F)$ ν_1 (10615 cm⁻¹), $^3A_{2g}(F) \rightarrow ^3T_{1g}(F)$ ν_2 (18248 cm⁻¹) and $^3A_{2g}(F) \rightarrow ^3T_{1g}(P)$ ν_3 (23923 cm⁻¹) d-d transitions respectively, which are strongly favoured for the octahedral geometry and also the observed magnetic moment value of Ni (II) complex is

2.9-3.4 BM, which is confirmed the octahedral geometry. The d-d transition favours octahedral geometry around the metal ion and the data were summarized in Table 2. The calculated Dq values of Ni (II) and Co (II) complexes are in the range of 608-1062 cm^{-1} which is suggested as a weak field ligand. The values of Racah inter electronic repulsion parameter (B) for the complexes are always less than the corresponding free ion B_0 value. The observed B (complex) values are less B_0 (free ion) which is indicated that the ligand is coordinated to the metal ion and Dq values for the Ni (II) and Co (II) complexes were also calculated from the equation $Dq = [v_1/10]$ and $[v_2-v_1/10]$ respectively. If the value of Nephelauxetic parameter (β) is equal to unity or greater than unity ($\beta > 1$), it is indicated the greater ionic character of M-L bond. The observed β values of the complexes were less than unity ($\beta < 1$), was suggested the greater covalency of the M-L bond. The observed value of β_0 value of (v_2/v_1) ratio is in the range of 1.60 – 1.72 which is considered as an identification of octahedral geometry in the Ni (II) and Co (II) mixed ligand complexes. The LFSE values were calculated from the equations $\text{LFSE} = 12 Dq$ for Ni (II) and $6 Dq$ for Co (II) complexes. The ligand field parameters and magnetic values have been proposed that an octahedral geometry [38].

Table 2 Electronic absorption spectral data of the complexes

Complex	Abs. Region cm^{-1} (λ_{max})	Band assignment	Ligand Field parameter							Suggested Geometry
			Dq cm^{-1}	B cm^{-1}	β cm^{-1}	β_0 (%)	v_2/v_1 cm^{-1}	LFSE K Cal	Dq/B	
[HL]	25062 (399) 31746 (315) 39370 (254)	INCT INCT	-	-	-	-	-	-	-	---
[CoLX] 4H ₂ O	10204 (980) 16340 (612) 25062 (399)	$^4T_{1g}(F) \rightarrow ^4T_{2g}(F) v_1$ $^4T_{1g}(F) \rightarrow ^4A_{2g}(F) v_2$ $^4T_{1g}(F) \rightarrow ^4T_{1g}(P) v_3$	614	719	0.70	30	1.60	36.8	0.85	Octahedral
[NiLX] 4H ₂ O	10615 (942) 18248 (548) 23923 (418)	$^3A_{2g}(F) \rightarrow ^3T_{2g}(F) v_1$ $^3A_{2g}(F) \rightarrow ^3T_{1g}(F) v_2$ $^3A_{2g}(F) \rightarrow ^3T_{1g}(P) v_3$	1062	688	0.71	29	1.72	12.7	1.54	Octahedral
[CoLY] 4H ₂ O	10132 (987) 16207 (617) 24390 (410)	$^4T_{1g}(F) \rightarrow ^4T_{2g}(F) v_1$ $^4T_{1g}(F) \rightarrow ^4A_{2g}(F) v_3$ $^4T_{1g}(F) \rightarrow ^4T_{1g}(P) v_3$	608	680	0.66	34	1.60	36.5	0.89	Octahedral
[NiLY] 4H ₂ O	10256 (975) 16474 (607) 26316 (380)	$^3A_{2g}(F) \rightarrow ^3T_{2g}(F) v_1$ $^3A_{2g}(F) \rightarrow ^3T_{1g}(F) v_2$ $^3A_{2g}(F) \rightarrow ^3T_{1g}(P) v_3$	1026	801	0.82	18	1.61	12.31	1.28	Octahedral

Where INCT = intra ligand charge transfer band

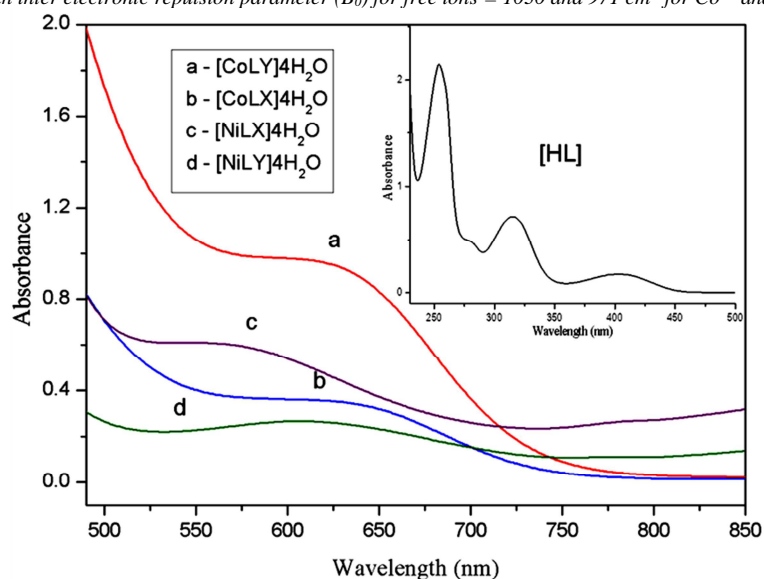
*Racah inter electronic repulsion parameter (B_0) for free ions = 1030 and 971 cm^{-1} for Co^{2+} and Ni^{2+} .

Figure 2 Electronic absorption spectra of mixed ligand complexes and ligand peak (inset)

3.3 IR Spectroscopy

The IR spectrum of the ligand is showed the characteristic $\nu(-CH=N)$ bands in the region 1630 cm^{-1} , which is shifted to lower frequencies in the spectra of all the complexes ($1620\text{--}1598\text{ cm}^{-1}$) indicating the involvement of $-CH=N$ nitrogen in coordination to the metal ion [39-40]. The ligand is showed a broad band in the region 3210 cm^{-1} , assignable to phenolic $-OH$ groups, which is absent in the spectra of the all metal complexes suggest confirming the disappearance of phenolic proton and oxygen atom involved in the formation of $M-O$ bond. Morpholine $\nu(C-N-C)$ band is appeared in the region 1375 cm^{-1} , which is shifted to lower frequencies in the spectra of all the complexes ($1355\text{--}1338\text{ cm}^{-1}$) indicating the involvement of $C-N-C$ nitrogen in coordination to the metal ion. The IR spectra are evident that the ligand acts as tridentate chelating agent. In all complexes, carboxylate of the acetate group is strongly absorbed (ν_{asy}) in the range of $1667\text{--}1662\text{ cm}^{-1}$ and (ν_{sym}) more weakly at $1404\text{--}1399\text{ cm}^{-1}$ (Table 3). It is suggested that they are consisting of unidentate co-ordination site due to the value of differences between asymmetry and symmetry is greater than 200 cm^{-1} ($\Delta\nu_{a-s} \geq 200\text{ cm}^{-1}$). The spectra of the metal chelates is also showed new bands in the region $659\text{--}617\text{ cm}^{-1}$ and $497\text{--}483\text{ cm}^{-1}$, which are indicated the formation of $\nu(M-O)$ and $\nu(M-N)$ bonds.

Table 3 IR spectral data of the synthesized compounds

Complex	$\nu(C=N)$	$\nu(C-O)$	Ali- $\nu(C-O-C)$	Ali- $\nu(C-N-C)$	Ph-OH $\nu(O-H)$	ν (Acetate)	ν (H_2O)	Co-ligand (X/Y) $\nu(C=N)$	$\nu(M-O)$	$\nu(M-N)$
[HL]	1630	1200	1146	1375	3210	-	-	-	-	-
[CoLX] 4H ₂ O	1620	1223	1143	1338	-	1662(a) 1401(s)	860	1570	653	492
[NiLX] 4H ₂ O	1622	1229	1139	1349	-	1665(a) 1404(s)	845	1558	659	483
[CoLY] 4H ₂ O	1598	1232	1140	1340	-	1664(a) 1399(s)	855	1569	617	497
[NiLY] 4H ₂ O	1616	1229	1134	1355	-	1667(a) 1400(s)	840	1565	657	487

Where a-asymmetry and s-symmetry

3.4 Redox studies

Cyclic voltammogram of the cobalt and nickel complexes were recorded in ethanol solution (potential range 1.0 to -1.0 V) show a well-defined redox process (Figure 3 (a) and (b)) corresponding to the formation of $Co(II)/Co(I)$ couple and $Ni(II)/Ni(I)$ couple. The $[CuLX]4H_2O$ and $[NiLX]4H_2O$ complexes display a reversible voltametric cathodic peak at 0.11 and 0.14 V and reversible anodic peak at -0.25 and -0.29 V. The quasi-reversible peak is obtained for the copper complexes of 0.14 and 0.15 V respectively at a scan rate of 100 mVs^{-1} . In addition, the ratio of anodic and cathodic peak current ($I_p/I_{p_a} \approx 1$) is being corresponded to one electron transfer process (Table 4).

Table 4 Cyclic voltammogram data of the mixed ligand complexes (0.001M) in ethanol at 300 K in ethanol containing 0.1M (TBAP). Scan rate 100 mVs^{-1}

Complex	Couple	E_{pc} (V)	E_{pa} (V)	ΔE_p (V)	I_{pa} (μA)	I_{pc} (μA)	I_{pa}/I_{pc}
[CoLX]4H ₂ O	$Co(II)/Co(I)$	0.11	-0.25	0.14	-2.89	2.92	0.99
[NiLX]4H ₂ O	$Ni(II)/Ni(I)$	0.14	-0.29	0.15	-2.74	2.90	0.95

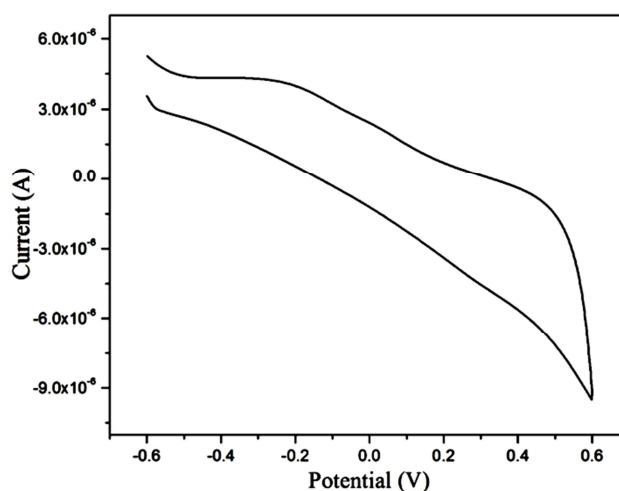


Figure 3 (a) The cyclic voltammogram of the $[NiLX]4H_2O$ complex in ethanol at 300 K

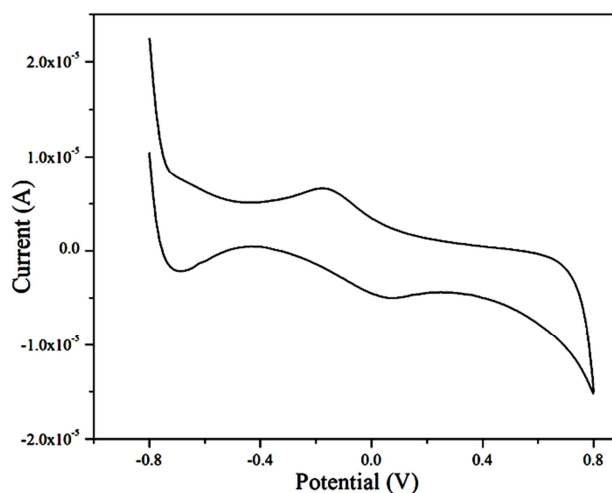


Figure 3 (b) The cyclic voltammogram of the [CoLX]4H₂O complex in EtOH at 300 K

3.5 DNA binding studies

3.5.1 Electronic Absorption method

Absorption titration is employed to determine the binding mode and binding strength of the complexes with DNA. Transition metal complexes can be bound to DNA via covalent and/or non-covalent interactions (intercalative, electrostatic and groove binding). Complex bind to DNA through intercalation usually results in hypochromism (decrease in absorbance) and bathochromism (red shift), because intercalative mode involves a strong stacking interaction between aromatic chromophore and the base pairs of DNA [41]. Electrostatic interaction of complex with DNA is showed the lower hypochromicity with no bathochromic shift [42]. Complex binds to DNA through covalent binding generally results in hyperchromism resulting from breakage of secondary structure of DNA due to the fact that phosphate group can be provided the suitable anchors for coordination with complexes. The extent of hyperchromism is also revealed the nature of binding affinity. The absorption spectrum of Co(II) and Ni(II) complexes with increasing concentration of HS-DNA is shown in Figure 4 (a), (b), (c) & (d). As the concentration of DNA increases, hypochromism is observed in the charge transfer band of each complex along with the red shift of about 2-5 nm which is suggested to the covalent binding of metal complexes with DNA. The K_b values were calculated from the perturbation observed in charge transfer band of the complexes. The absorption data was analyzed to evaluate the intrinsic binding constant (K_b), which can be determined from a plot of $[DNA]/(\epsilon_a - \epsilon_f)$ versus $[DNA]$ using the following equation [43].

$$\frac{[DNA]}{(\epsilon_a - \epsilon_f)} = \frac{[DNA]}{(\epsilon_b - \epsilon_f)} + \frac{1}{K_b(\epsilon_b - \epsilon_f)}$$

Where $[DNA]$ is the concentration of HS-DNA in base pairs. The apparent absorption coefficients ϵ_a , ϵ_f and ϵ_b correspond to $A_{\text{obsd}}/[M]$, the extinction coefficient for the metal(II) complex in fully bound form respectively. K_b is given by the ratio of slope to the intercept. The lower K_b values can be accredited to non-planarity of substituent which might be caused the severe steric constraints near the metal core when the complex approaches the DNA base pairs. The values of K_b in Table 5 clearly show that the [CoLX]4H₂O have more DNA-binding activity compared to [CoLY]4H₂O, [NiLX]4H₂O and [NiLY]4H₂O complexes. The calculated intrinsic binding constant (K_b) and free energy change (ΔG_b°) of mixed ligand complexes are presented in Table 5. The negative free energy changes observed in all cases indicate that the complexes interact with DNA in a spontaneous manner [44-46].

Table 5 Intrinsic binding constant (K_b) and free energy change (ΔG_b°) of mixed ligand complexes

Complex	$\lambda_{\text{max}}(\text{nm})$		$\Delta\lambda$ (nm)	Chromism (H%)	Binding constant $K_b \times 10^3 (\text{M}^{-1})$	Type of Chromism & shift	ΔG_b° (kJ M^{-1})
	Free	Bound					
[CoLX]4H ₂ O	394	399	5	84.91	8.04	Hypo & red	-53.73
[NiLX]4H ₂ O	306	309	3	23.13	7.10	Hypo & red	-50.53
[CoLY]4H ₂ O	388	391	3	11.17	4.17	Hypo & red	-36.81
[NiLY]4H ₂ O	306	308	2	41.88	6.79	Hypo & red	-49.38

$$H\% = [(A_{\text{free}} - A_{\text{bound}}) / A_{\text{free}}] 100\%$$

K_b = Intrinsic binding constant determined from the UV-Vis. absorption spectral titration.

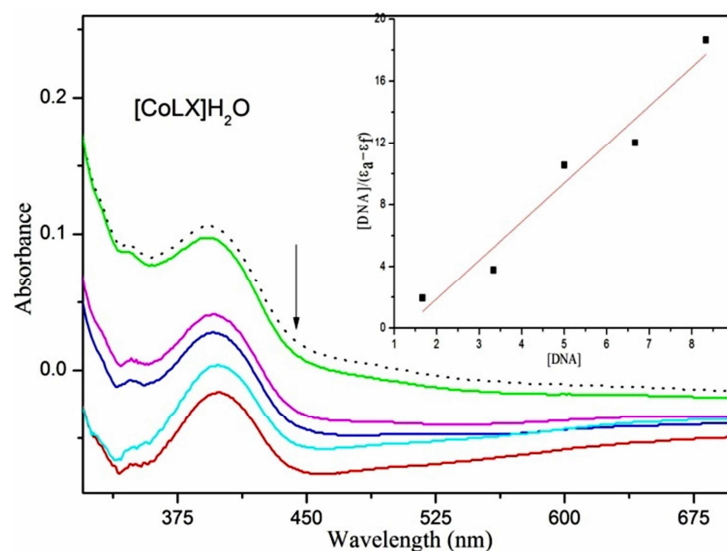


Figure 4 (a) Electronic spectra of $[\text{CoLX}]_4\text{H}_2\text{O}$ in Tris-HCl buffer upon addition of HS-DNA. $[\text{Complex}] = 30 \mu\text{M}$, $[\text{DNA}] = 0-50 \mu\text{M}$. Dotted line shows free complex and thick line shows complex upon addition of $[\text{DNA}]$

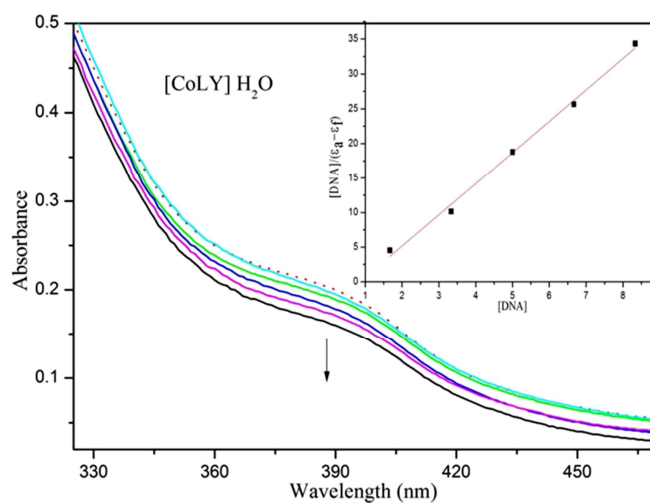


Figure 4 (b) Electronic spectra of $[\text{CoLY}]_4\text{H}_2\text{O}$ in Tris-HCl buffer upon addition of HS-DNA. $[\text{Complex}] = 30 \mu\text{M}$, $[\text{DNA}] = 0-50 \mu\text{M}$. Dotted line shows free complex and thick line shows complex upon addition of $[\text{DNA}]$

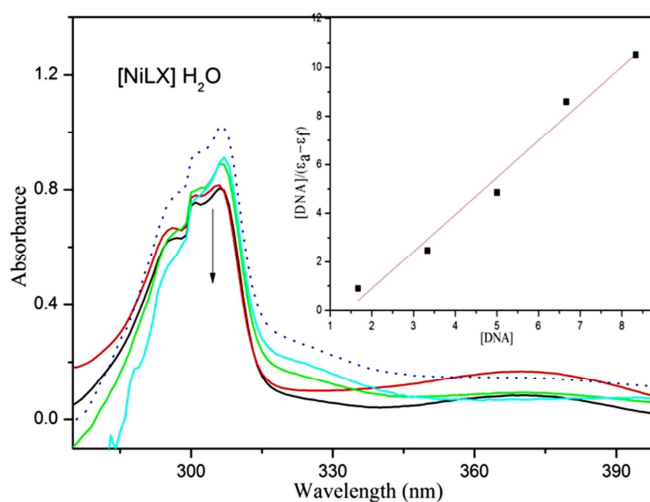


Figure 4 (c) Electronic spectra of $[\text{NiLX}]_4\text{H}_2\text{O}$ in Tris-HCl buffer upon addition of HS-DNA. $[\text{Complex}] = 30 \mu\text{M}$, $[\text{DNA}] = 0-50 \mu\text{M}$. Dotted line shows free complex and thick line shows complex upon addition of $[\text{DNA}]$

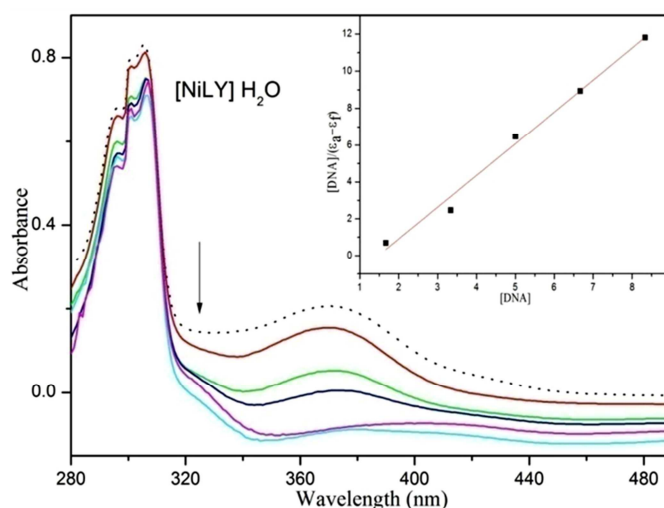


Figure 4 (d) Electronic spectra of $[\text{NiLY}]4\text{H}_2\text{O}$ in Tris-HCl buffer upon addition of HS-DNA. $[\text{Complex}] = 30 \mu\text{M}$, $[\text{DNA}] = 0-50 \mu\text{M}$. Dotted line shows free complex and thick line shows complex upon addition of $[\text{DNA}]$

3.5.2 Viscosity titration measurement

As a means for further clarifying the binding of the Co and Ni complexes, viscosity measurements were carried out on HS DNA by varying the concentration of the added complexes. Hydrodynamic measurements which are sensitive to length increase are regarded as the least ambiguous and the most critical tests of binding in solution in the absence of crystallographic structure data [47]. A classical intercalative mode causes a significant increase in separation of base pairs at intercalation sites and hence an increase in overall DNA length. By contrast, complexes that binds exclusively in the DNA grooves by partial and/or non-classical intercalation, under the same conditions, typically cause less pronounced or no change in DNA solution viscosity [48]. The values of $(\eta/\eta_0)^{1/3}$ were plotted against $[\text{complex}]/[\text{DNA}]$ (Figure 5). The results reveal that all the complexes exhibit increase in relative viscosity of DNA, which suggest all the complexes bind to DNA by intercalation [49].

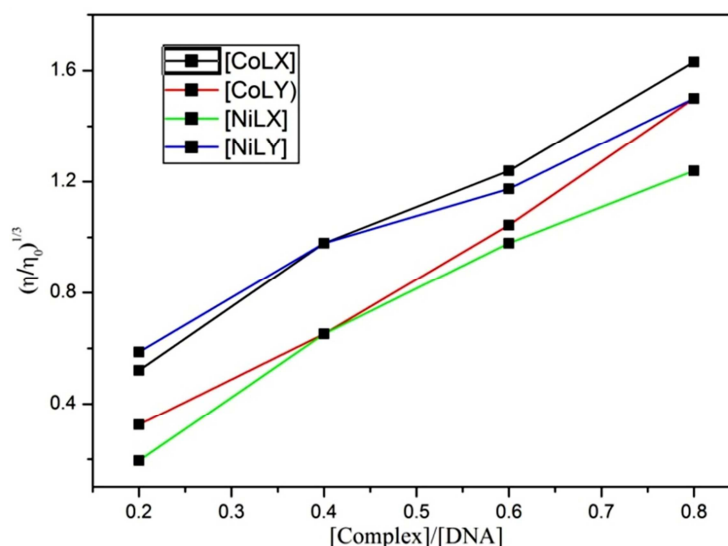
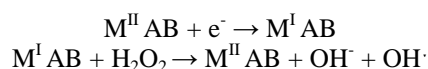


Figure 5 Effect of increasing amounts of complexes on the relative viscosities of HS DNA

3.7 DNA Cleavage activity

The CT-DNA cleavage study by gel electrophoresis method was performed with mixed ligand complexes at 37°C . The cleavage properties were studied in a medium of 50 mM Tris-HCl/NaCl buffer ($\text{pH} = 7.2$) in the presence of H_2O_2 . Bromophenol blue was used as a photosensitizer. The DNA cleavage efficiency of the complex depends on its different attaching capacity to DNA. The observed electrophoretic results (Figure 6) conclude that $[\text{NiLX}]4\text{H}_2\text{O}$ (lane 4) and $[\text{CoLY}]4\text{H}_2\text{O}$ (lane 5) complexes cleave the DNA appreciably as compared to the control DNA while $[\text{CoLX}]4\text{H}_2\text{O}$ (lane 3), $[\text{NiLY}]4\text{H}_2\text{O}$ (lane 6) and ligand (lane 2) fail to include any significant cleavage on DNA even on long exposure time. It is also observed that free radical scavengers inhibited the DNA cleavage which confirms the involvement of free radical. On the basis, a general radical oxidative mechanism is proposed for DNA

cleavage. It is believed that the DNA cleavage by metal complexes arises as a result of attack of diffusible hydroxyl radical (OH^\cdot) on DNA through Fenton type mechanism as reported earlier. The hydroxyl free radical is formed a result of reaction between the complex and the oxidising agent, H_2O_2 via Fenton or Haber-Weiss mechanism [50]. According to the Fenton mechanism, the complex acts as a catalyst for hydroxyl radical generation from H_2O_2 [51].



The hydroxyl free radical abstracts a hydrogen atom from sugar moiety of DNA to form sugar radical. These sugar radicals then undergo hydrolytic cleavage at sugar-phosphate backbone to release specific residues depending on the position from which the hydrogen atom is being removed. Further, it was reported that when DNA is run through agarose gel during electrophoresis, the fastest migration was observed for the open circular form. The considerable activity for DNA cleavage found with mixed ligand complexes containing Co(II) and Ni(II) compared with that of the control may also be partially due to the ability of these complexes to convert open circular DNA into its linear form.

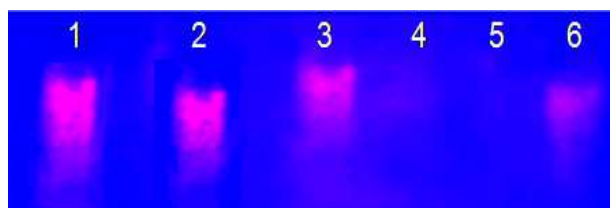


Figure 6 The nuclease activity of present complexes, investigated on CT DNA by agarose gel electrophoresis in the presence of oxidant (H_2O_2)

Lanes right to left → Lane 1, CT DNA alone; Lane 2, DNA + [HL]; Lane 3, DNA + [CoLX] $4\text{H}_2\text{O}$ + H_2O_2 ; Lane 4, DNA + [NiLX] $4\text{H}_2\text{O}$ + H_2O_2 ; Lane 5, DNA + [CoLY] $4\text{H}_2\text{O}$ + H_2O_2 ; Lane 6, DNA + [NiLY] $4\text{H}_2\text{O}$ + H_2O_2 .

3.8 DPPH Radical Scavenging studies

Antioxidant activities of mixed ligand complexes were ascertained by DPPH free radical scavenging assay. This method depends on the ability of the antioxidant to donate its electron to DPPH which in turn depends on the ability of 1,1-diphenyl-2-picryl-hydrazyl (DPPH) to change color from purple to yellow. From the results, it is shown that the mixed ligand complexes have higher activities than ligand (Table 6) which may be due to the presence of the M(II) ion moiety in the complex [52]. In addition, the antioxidant activities of these complexes are given in Figure 7 and 8.

$$\text{Scavenging effects (\%)} = \left[\frac{(A_{\text{control}} - A_{\text{sample}})}{A_{\text{control}}} \right] \times 100$$

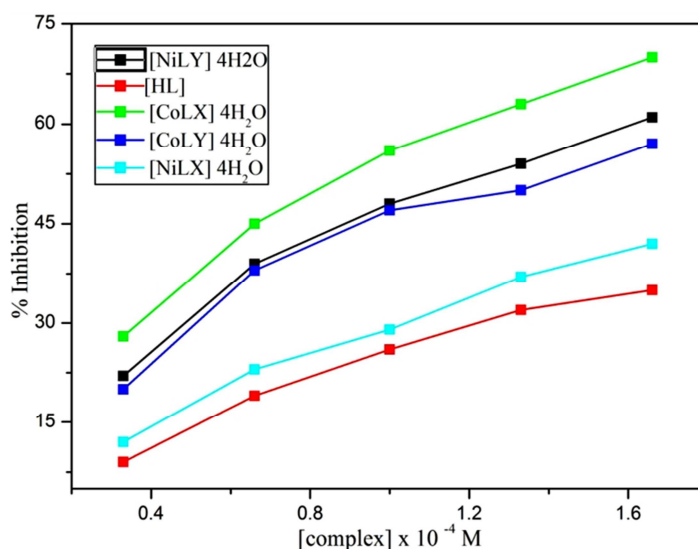
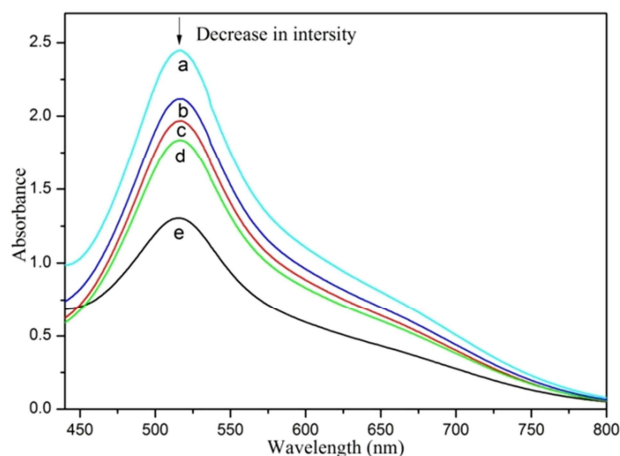


Figure 7 Electronic absorption spectrum of DPPH free radical scavenging activity for mixed ligand complexes

Table 6 *In vitro* antioxidant of activities of ligand and its mixed ligand complexes at different concentraion by DPPH free radical scavenging assay method

Complex	Scavenging activity (%)				
	10 μ M	20 μ M	30 μ M	40 μ M	50 μ M
[HL]	9	19	26	32	35
[CoLX]4H ₂ O	28	45	59	68	78
[CoLY]4H ₂ O	20	38	47	50	57
[NiLX]4H ₂ O	12	23	29	37	42
[NiLY]4H ₂ O	22	39	48	54	61

**Figure 8** Electronic absorption spectra of a= [HL], b= [NiLX]4H₂O, c= [CoLY]4H₂O, d= [NiLY]4H₂O and e= [CoLX]4H₂O by DPPH free radical scavenging method at a concentration of 100 μ M

3.9 Antimicrobial activity

The *in vitro* antimicrobial activity of the investigated compounds were tested against the bacteria *Salmonella typhi*, *Escherichia coli*, *Bacillus subtilis*, *Staphylococcus aureus*, *Streptococcus faecalis*, *Salmonella typhimurim*, *Klebsiella pneumonia* and fungi *Shigella boydii*, *Candida albicans*, *Aspergillus niger* by well diffusion method. The sensitivity of microorganisms to antimicrobial complex was measured as inhibition zone (mm) are summarized in Table 7. A comparative study of the ligand and its mixed ligand complexes (inhibition zone values) indicates that complexes exhibit higher antimicrobial activity than the free ligand is given in Figure 9. From the inhibition zone values, it was found that the mixed ligand complexes were more potent than ligand. Further studies are required to explore these complexes as drugs. Such increased activity of the complexes can be explained on the basis of Overtone's concept [53] and Tweedy's Chelation theory [54]. According to Overtone's concept of cell permeability, the lipid membrane that surrounds the cell favors the passage of only the lipid-soluble materials due to which liposolubility is an important factor, which controls the antifungal activity. On chelation, the polarity of the metal ion will be reduced to a greater extent due to the overlap of the ligand orbital and partial sharing of the positive charge of the metal ion with donor groups. Furthermore, the mode of action of the compound may be involved the formation of a hydrogen bond through the azomethine group with the active centre of cell constituents, resulting in interference with the normal cell process.

Table 7 Antibacterial activity of the Schiff base ligand and its mixed metal complexes

Complex	Gram positive bacteria			Gram negative bacteria				Fungi	
	B	C	D	E	F	G	H	I	J
[HL]	7.7	8.4	10.2	11.5	7.2	15.7	10.6	11.3	10.2
[CoL]4H ₂ O	18.6	16.6	17.4	21.4	12.3	18.8	19.3	15.8	17.4
[NiL]4H ₂ O	20.3	22.2	18.6	22.9	18.6	20.5	20.3	19.7	18.6
[CoLX]4H ₂ O	15.7	21.4	20.3	17.3	15.1	22.7	20.2	19.2	24.3
[NiLX]4H ₂ O	19.3	20.2	20.4	21.3	18.5	20.6	19.8	21.3	22.4
[CoLY]4H ₂ O	17.7	19.4	20.4	17.5	19.1	20.6	20.2	19.3	22.5
[NiLY]4H ₂ O	20.3	20.2	20.7	21.5	18.5	22.6	18.8	20.3	21.4
Streptomycin	28.7	27.2	28.7	26.1	27.4	25.5	27.3	28.7	28.6

B = *S. aureus*, C = *B. subtilis*, D = *S. faecalis*, E = *E. coli*, F = *S. typhimurim*, G = *K. pneumonia*, H = *S. boydii*, I = *C. albican* and J = *A. niger*

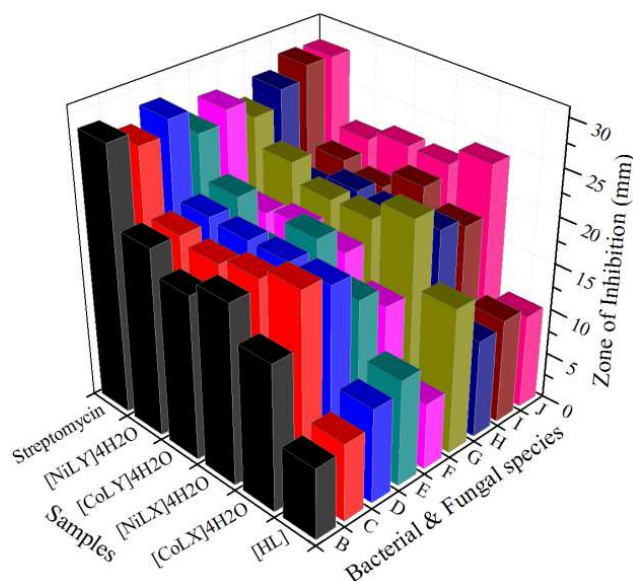


Figure 9 Antibacterial and antifungal activities of complexes at a concentration of 10^{-2} M determined by well diffusion method

CONCLUSION

A new tridentate schiff base ligand N_2 type was derived from the condensation of 3-morpholinopropyl amine and salicylaldehyde. Four mixed ligand complexes containing Co(II) and Ni(II) and ligand were synthesized and characterized by spectral and analytical techniques. From the study it has been concluded that the ligand bind to the M(II) ions through two N (imine & morpholine ring) and phenolic C-O atoms. The data is showed that the mixed ligand complexes have the composition of type $[MLX]4H_2O$ and $[MLY]4H_2O$. The UV-Vis spectral data suggest that these complexes exhibit octahedral geometry. They have showed low electrical conductance which reveals that the chelates are non-electrolytes. Their magnetic susceptibility values are provided evidence for the monomeric nature. The measurement of DNA binding affinity of mixed ligand complexes towards HS-DNA using absorption spectral analysis is suggested the highest K_b value for complex $[CoLX]4H_2O$. The binding of M(II) complexes with DNA has been confirmed from a red shift along with a decrease in intensity of the charge transfer band (hypochromicity). The spontaneous nature of binding between complex and DNA was inferred from the negative free energy value calculated from K_b value. The results from absorption spectral and viscosity studies revealed that all the complexes can bind to DNA by intercalation through the covalent binding mode of interaction. Further, the interaction of the complexes with CT-DNA was investigated by gel electrophoresis. The presence of a smear in the gel diagram indicates the presence of radical cleavage. The DNA cleavage activity of $[CoLX]4H_2O$ and $[NiLY]4H_2O$ complexes with CT-DNA demonstrated remarkable activity, while $[CoLY]4H_2O$, $[NiLX]4H_2O$ complexes and ligand (HL) showed no activity under aerobic condition and in the presence of H_2O_2 . The *in vitro* biological and antioxidant studies have shown that the mixed ligand complexes have higher potent activities than the free ligand. The higher activity of complexes exhibited against bacterial and fungal strains have been interpreted on the basis of the presence of both electron withdrawing and electron donating moieties in the chelate ring.

Acknowledgements

The authors express their sincere and heartfelt thanks to the Department of Science and Technology (DST) – Science and Engineering Research Board (SERB-Ref. SR/FT/CS-117/2011 dated 29.06.2012), Government of India, New Delhi for their funding assistance, the Managing Board, Principal and Chemistry Research Centre of Mohamed Sathak Engineering College, Kilakarai. The authors thank the Managing Board and Principal of Sri Vidya College of Engineering & Technology, Virudhunagar and V.O.C College of Arts & Science, Tuticorin for providing all the research and instrumental facilities. The authors also thank the SAIF, IIT Bombay, STIC CUSAT, Cochin.

REFERENCES

- [1] K Siddappa; SB Mane; D Manikprabhu. *Spectrochim. Acta A*, **2014**, 130, 634.
- [2] ML Sundararajan; T Jeyakumar; J Anandakumaran; BK Selvan. *Spectrochim. Acta A*, **2014**, 131, 82.
- [3] RM Ramadan; AK Abu Al-Nasr; FH Noureldeen. *Spectrochim. Acta A*, **2014**, 132, 417.
- [4] SK Sridhar; M Saravanan; A Ramesh. *Eur. J. Med. Chem.* **2001**, 36, 615-625.
- [5] S Chandra; M Pundir. *Spectrochim. Acta A*, **2008**, 69, 1.

- [6] K Dhahagani; SM Kumar; G Chakkaravarthi; K Anitha; J Rajesh; A Ramu; G Rajagopal. *Spectrochim. Acta A* **2014**, 117, 87.
- [7] P Majumdar; AK Ghosh; LR Falvello; SM Peng; Goswami. *Inorg. Chem.* **1998**, 37, 1651.
- [8] MG Verma; VR Sharma; AK Saxena; TN Bhalla; JN Sinha; KP Bhargava et al., *Pharmacol. Res. Commun.* 16, 9.
- [9] S Chandra; LK Gupta; S Agrawal. *Trans. Met. Chem.* **2007**, 32, 558.
- [10] Kathrin Wahlar; Anja Ludewig; Patrick Szabo; Klaus Harms; Eric Meggers. *Eur. J. Inorg. Chem.* **2014**, 5, 807.
- [11] SK Padhi; R Sahu; V Manivannan. *Polyhedron*, **2008**, 27, 805.
- [12] Y Liu; N Wang; W Mei; F Chen; H Li-Xin; L Jian; R Wang. *Trans. Met. Chem.* **2007**, 32, 332.
- [13] BO West. *Chemistry of Coordination Compounds of Schiff bases in New pathways in Inorganic chemistry*, Eds. Ebsworth EAV, Sharpe AG, Cambridge University Press, **1968**, p. 303.
- [14] P Mukherjee; MGB Drew; V Tangoulis; M Estrader; C Diaz; A Ghosh. *Polyhedron*, **2009**, 28, 2989.
- [15] PJ Steel. *Coord. Chem. Rev.* **1990**, 106, 227.
- [16] R Vijayalakshmi; M Kanthimathi; V Subramanian; BU Nair. *Biochem. Biophys. Acta*, **2000**, 1475, 157.
- [17] KS Ksaprak. *Chem. Res. Toxicol.* **1991**, 4, 604.
- [18] A Kamal; R Ramu; V Tekumalla; GBR Khanna; MS Barkume; AS Juvekarb; SM Zingde. *Bioorg. Med. Chem.* **2007**, 15, 6868.
- [19] SA Bourne; J Lu; A Mondal; B Moulton; MJ Zaworotko. *Angew. Chem. Int.* **2001**, Ed. 40, 2111.
- [20] C Sissi; F Mancin; M Gatos; M Palumbo; P Tecilla; U Tonellato. *Inorg. Chem.* **1999**, 44, 2310.
- [21] ST Frey; HHJ Sun; NN Murthy; KD Karlin. *Inorg. Chim. Acta*, **1996**, 242, 329.
- [22] DD Perrin; WLF Armarego; DR Perrin; *Purification of Laboratory Chemicals*, Pergamo Press, Oxford, **1980**.
- [23] J Marmur. *J. Mol. Biol.* **1961**, 3, 208.
- [24] ME Reichmann; SA Rice; CA Thomas; P Doty. *J. Am. Chem. Soc.* **1954**, 76, 3047.
- [25] A Wolfe; GH Shimer; T Meehan. *Biochemistry*, **1987**, 26, 6392.
- [26] S Satyanarayana; JC Daborusak; JB Chaires. *Biochemistry*, **1993**, 32, 2573–2584.
- [27] MS Blois. *Nature*, **1958**, 4617 (181), 1199-1200.
- [28] MJ Pelczar; ECS Chan; NR Krieg. *Microbiology*, 5th Edn. **1998**, New York.
- [29] N Kannan. *Laboratory Manual in Microbiology 1st Edn.* Paramount Publication, **1996**, Palani.
- [30] WJ Geary. *Coord. Chem. Rev.* **1971**, 7, 81-122.
- [31] BJ Hathaway; DE Billing; P Nicholls; IM Procter. *J. Chem. Soc. (A)*, **1969**, 319.
- [32] BJ Hathaway; IM Procter; RC Slade; AAG Tomlinson. *J. Chem. Soc. (A)*, **1969**, 2219.
- [33] H Okawa; DH Busch. *Inorg. Chem.* **1979**, 18, 1555.
- [34] ABP Lever; E Mantovani. *Inorg. Chem.* **1971**, 10, 817.
- [35] M Calligaris; G Nardin; L Randaccio; A Ripaamonti. *J. Chem. Soc. (A)*, **1970**, 1069.
- [36] Y Nishida; S Kida. *Bull Chem. Soc. Jpn.* **1978**, 51, 143.
- [37] AL Crumbliss; F Basolo. *J. Am. Chem. Soc.* **1970**, 92, 55.
- [38] ABP Lever. *Inorganic electronic spectroscopy*, 2nd edition, **1968**, New York.
- [39] JL Lamboy; A Pasquale; AL Rheingold; E Meléndez. *Inorg. Chim. Acta*, **2007**, 360, 2115.
- [40] AG de A Fernandes; PI de S Maia; J de Souza; SS Lemos; AA Batista; U Abram; J Ellena; EE Castellano; VM Deflon. *Polyhedron*, **2008**, 27, 2983.
- [41] Nahid Shahabadi; Soheila Kashanian; Mehdi Purfoulad. *Spectrochim. Acta. Part A*, **2009**, 72, 757.
- [42] R Indumathy; M Kanthimathi; T Weyhermuller; BU Nair. *Polyhedron*, **2008**, 27, 3443.
- [43] CS Allardyce; PJ Dyson; DJ Ellis; SL Heath. *Chem. Commun.* **2001**, 1396.
- [44] J Dharmaraja; T Esakkidurai; P Subbaraj; Sutha Shobana. *Spectrochim. Acta*, **2013**, 114A, 607-621.
- [45] Shobana; P Subramaniam; J Dharmaraja; S Arvindnarayan. *Spectrochim. Acta*, **2014**, 126A, 242-253.
- [46] S Zang; J Zhou. *J. Coord. Chem.* **2008**, 61(15), 2488-2498.
- [47] BC Beguley; M LeBret. *Biochemistry*, **1984**, 23, 937.
- [48] TM Kelly; AB Tossi; DJ McConnell; TC Strekas. *Nucleic acids Res.* **1985**, 13, 6017.
- [49] F Liu; KA Meadows; DR McMillan. *J. Am. Chem. Soc.* **1993**, 115, 6699.
- [50] A Charles; III Detmer; V Filomena; Pamatong, R Jaffery, Bocarcly. *Inorg. Chem.* **1996**, 35, 6292-6298.
- [51] TD Tullus. (Ed.), *Metal-DNA Chemistry*, ACS Symposium Series 402, American Chemical Society, Washington, DC, **1989**.
- [52] MS Blois. *Nature*, **1958**, 181, 4617, 1199-1200.
- [53] Y Ding; XX Hu; XL Sun; ZL Zuo. *J. Natural Science*, **2010**, 15, 165.
- [54] N Dharamaraj; P Viswanathamurthi; K Natarajan. *Trans. Met. Chem.* **2001**, 26, 105.